Control of the pericentrosomal H_2O_2 level by peroxiredoxin I is critical for mitotic progression

Jung Mi Lim,[1] Kyung S. Lee,[2] Hyun Ae Woo,[1] Dongmin Kang,[1] and Sue Goo Rhee[3]

[1]Division of Life and Pharmaceutical Sciences, Ewha Womans University, Seoul 120-750, South Korea
[2]Laboratory of Metabolism, National Cancer Institute, Bethesda, MD 20892
[3]Yonsei Biomedical Research Institute, Yonsei University, Seoul 120-749, South Korea

Proteins associated with the centrosome play key roles in mitotic progression in mammalian cells. The activity of Cdk1-opposing phosphatases at the centrosome must be inhibited during early mitosis to prevent premature dephosphorylation of Cdh1—an activator of the ubiquitin ligase anaphase-promoting complex/cyclosome—and the consequent premature degradation of mitotic activators. In this paper, we show that reversible oxidative inactivation of centrosome-bound protein phosphatases such as Cdc14B by H_2O_2 is likely responsible for this inhibition. The intracellular concentration of H_2O_2 increases as the cell cycle progresses. Whereas the centrosome is shielded from H_2O_2 through its association with the H_2O_2-eliminating enzyme peroxiredoxin I (PrxI) during interphase, the centrosome-associated PrxI is selectively inactivated through phosphorylation by Cdk1 during early mitosis, thereby exposing the centrosome to H_2O_2 and facilitating inactivation of centrosome-bound phosphatases. Dephosphorylation of PrxI by okadaic acid–sensitive phosphatases during late mitosis again shields the centrosome from H_2O_2 and thereby allows the reactivation of Cdk1-opposing phosphatases at the organelle.

Introduction

Activation of the Cdk1–cyclin B complex occurs first at the centrosome during prophase, and its amplification through multiple feedback loops involving cyclin B, Cdc25B, Cdc25C, Plk, and Aurora A also occurs at this organelle (Jackman et al., 2003; Bonnet et al., 2008; Lindqvist et al., 2009). Successful cell cycle progression requires that many cell cycle regulators—including cyclins A and B, Plk1, and Aurora A—be degraded in a timely manner. Degradation of these regulators by the 26S proteasome results from their ubiquitination by the multisubunit ubiquitin ligase anaphase-promoting complex/cyclosome (APC/C). Activation of APC/C occurs at the centrosome and requires Cdc20 or Cdh1 as an activator protein (Peters, 2006; Pesin and Orr-Weaver, 2008; van Leuken et al., 2008; Wurzenberger and Gerlich, 2011). Cdh1 is prevented from interaction with APC/C when Cdh1 is phosphorylated by Cdks. APC/C–Cdh1 activity thus depends on both Cdks as well as Cdk-opposing phosphatases. The dual-specificity protein tyrosine phosphatase (PTP), Cdc14B, and the Ser/Thr phosphatases, PP1 and PP2A, have been proposed to function as Cdk1-opposing enzymes in mammalian cells (Bassermann et al., 2008; Mochida et al., 2009; Wu et al., 2009; Mocciaro and Schiebel, 2010; Schmitz et al., 2010; Domingo-Sananes et al., 2011).

A fraction of each of APC/C, Cdc20, Cdh1, and Cdk1-opposing phosphatases (Cdc14B, PP1, and PP2A) is present at the centrosome (Leach et al., 2003; Cho et al., 2005; Peters, 2006; Wu et al., 2008; Schmitz et al., 2010), as are Cdk1, Cdc25, cyclin B, Plk1, and Aurora A. At the onset of mitosis, Cdk1–cyclin B activity begins to increase as a result of positive feedback loops including cyclin B, Cdc25, Plk1, and Aurora A. The low level of incipient Cdk1 activity is likely insufficient to allow the accumulation of phosphorylated Cdh1 at the centrosome in the absence of concurrent suppression of the activity of Cdk1-opposing phosphatases, which, together with Cdh1, are enriched at this organelle. In the absence of such suppression of centrosomal phosphatase activity, further activation of Cdk1 would not be expected to occur because of the premature degradation of cyclin B, Plk1, and Aurora A.

Here, we find that the centrosomal levels of cyclin B, Plk1, and Aurora A as well as mitotic entry are likely regulated by the local concentration of H_2O_2 around the centrosome. We were led into this study by our previous observation that PrxI is inactivated when phosphorylated on Thr^{90} by purified Cdk1–cyclin B (Chang et al., 2002). Peroxiredoxins (Prxs) are a major class of H_2O_2-eliminating enzymes (Rhee et al., 2012). Mam-

Correspondence to Dongmin Kang: dkang@ewha.ac.kr; or Sue Goo Rhee: rheesg@yuhs.ac

Abbreviations used in this paper: APC/C, anaphase-promoting complex/cyclosome; DPI, diphenyleneiodonium; MAFP, methyl arachidonyl fluorophosphonate; MEF, mouse embryonic fibroblast; NDGA, nordihydroguaiaretic acid; NEM, *N*-ethylmaleimide; OA, okadaic acid; PACT, pericentrin-AKAP450 centrosomal targeting; pHH3, phosphorylated histone H3; Prx, peroxiredoxin; PTP, protein tyrosine phosphatase; SIM, structured illumination microscopy.

© 2015 Lim et al. This article is distributed under the terms of an Attribution–Noncommercial–Share Alike–No Mirror Sites license for the first six months after the publication date (see http://www.rupress.org/terms). After six months it is available under a Creative Commons License (Attribution–Noncommercial–Share Alike 3.0 Unported license, as described at http://creativecommons.org/licenses/by-nc-sa/3.0/).

The Rockefeller University Press $30.00
J. Cell Biol. Vol. 210 No. 1 23–33
www.jcb.org/cgi/doi/10.1083/jcb.201412068

THE JOURNAL OF CELL BIOLOGY

Downloaded from http://rupress.org/jcb/article-pdf/210/1/23/1590177/jcb_201412068.pdf by guest on 08 February 2026

malian cells express six Prx isoforms (PrxI to PrxVI), which are implicated in a variety of cellular processes.

Results and discussion

Phosphorylation of centrosome-associated PrxI in early mitotic cells

Whereas high H_2O_2 levels induce cell cycle arrest, low H_2O_2 levels are required for G_1–S and G_2–M phase transitions (Havens et al., 2006; Yamaura et al., 2009). The molecular mechanisms by which H_2O_2 modulates cell cycle progression have remained unclear, however. To examine the possible link between the role of H_2O_2 in cell cycle regulation and PrxI phosphorylation on Thr^{90}, we monitored this latter event during the cell cycle in HeLa cells that had been synchronized at the G_1–S border (0 h) with a double thymidine block and then released for various times. Phosphorylated PrxI (pPrxI) appeared slightly earlier than did the mitotic marker phosphorylated histone H3 (pHH3), and it disappeared in parallel with pHH3 (Fig. 1 A). When HeLa or U2OS cells arrested in prometaphase with nocodazole were released from the arrest, pPrxI disappeared rapidly, with the rate of its loss being slightly greater than that for cyclin B1 or pHH3 (Fig. S1 A).

The amount of pPrxI in prometaphase HeLa cells was estimated to be ∼0.4% of total PrxI (Fig. S1 B). We therefore reasoned that PrxI phosphorylation is likely a localized event, and we searched for its location in asynchronously growing HeLa cells using confocal microscopy. pPrxI was found to colocalize with the centrosome marker γ-tubulin at early stages of mitosis (prometaphase and metaphase) but not during interphase or late mitotic stages (anaphase, telophase, and cytokinesis; Fig. 1 B). The centrosome is composed of a pair of centrioles surrounded by pericentriolar material. Structured illumination microscopy (SIM; Fig. 1 C) revealed that although pPrxI is colocalized with Cep192, a pericentriolar material marker of mitotic cells (Kim et al., 2013), there are also regions of Cep192 that do not exhibit pPrxI. This may reflect unphosphorylated PrxI, although this remains to be verified. Release of HeLa cells from G_1–S arrest revealed that pPrxI was present at early and late prophase, prometaphase, and metaphase, but not during G_2, anaphase, telophase, or cytokinesis (Fig. S1 C). The appearance of pPrxI specifically at mitotic centrosomes was also detected in A431 and MCF7 cells (Fig. S1 D). The specificity of the antibodies to pPrxI was demonstrated using PrxI-deficient cells (Fig. S1, E and F). The centrosome-specific localization of pPrxI was also shown using biochemically isolated centrosomes (Fig. 1 D). Among the four cytosolic Prx enzymes (PrxI, II, V, and VI), only PrxI was detected at the centrosome (Fig. 1 D and Fig. S1 G).

When mouse embryonic fibroblasts (MEFs) were partially synchronized at mitosis and then released, the number of mitotic cells, estimated based on pHH3, was increased in PrxI-deficient MEFs compared with that in wild-type MEFs, and the levels of cyclin B1, Plk1, and Aurora A were higher in PrxI-deficient MEFs than in wild-type MEFs (Fig. S1 H).

Forced removal of pericentrosomal H_2O_2 by centrosome-targeted catalase inhibits mitotic entry

To examine the effect of exposure of the centrosome to cytoplasmic H_2O_2, which would be expected to occur as a result of PrxI phosphorylation (inactivation), we infected HeLa cells with a retroviral vector encoding a modified form of catalase either with a centrosome-targeting pericentrin-AKAP450 centrosomal targeting (PACT) sequence (Cat-PACT) or with the corresponding sequence lacking the centrosome-targeting core (Cat-delPACT; Fig. 2 A; Gillingham and Munro, 2000). The presence of Cat-PACT and the absence of Cat-delPACT at the centrosome were verified by confocal immunofluorescence microscopy (Fig. 2 B). HeLa cells that had been infected with the empty, Cat-PACT, or Cat-delPACT vectors were synchronized at G_1–S by thymidine treatment and released in the presence of nocodazole for 10 h (Fig. 2 C). Early mitotic cells were scored on the basis of cell rounding (Fig. 2 D) and chromosome condensation (Fig. 2 E). The number of mitotic cells (mean of values from Fig. 2, D and E) for cells expressing Cat-PACT was reduced by ∼45% and ∼35% compared with that for cells infected with the empty vector or the vector encoding Cat-delPACT, respectively. Immunoblot analysis of the infected HeLa cells showed that the level of inactive (Tyr^{15} phosphorylated) Cdk1 in Cat-PACT cells was about twice that in Cat-delPACT cells and that the level of pHH3 in Cat-PACT cells was ∼50% of that in Cat-delPACT cells (Fig. 2, F and G). Such analysis also revealed that Cat-PACT and Cat-delPACT were expressed stably at low levels relative to endogenous peroxisomal catalase, suggesting that any effect of Cat-PACT present in the cytosol instead of at the centrosome as a result of excessive expression was minimal (Fig. 2 F). We also monitored mitotic entry by fluorescence imaging of live cells after the release of Cat-PACT and Cat-delPACT cells from G_1–S arrest. Mitotic entry of Cat-PACT cells was delayed by a mean of ∼2–3 h compared with that of Cat-delPACT cells (Fig. 2 H; and Videos 1 and 2). These results thus supported the notion that exposure of the centrosome to H_2O_2 is required for normal mitotic entry.

We also found that the centrosomal levels of cyclin B1, Plk1, and Aurora A in Cat-PACT cells were reduced by 55, 30, and 40%, respectively, compared with those in Cat-delPACT cells, suggesting that exposure of the centrosome to H_2O_2 is likely required to protect them from degradation (Fig. 2, I–K).

Intracellular sources of H_2O_2 during mitosis

Reactive oxygen species including H_2O_2 increase gradually during cell cycle progression. There are multiple potential sources of H_2O_2 during mitosis, which include NADPH oxidase 4 (Yamaura et al., 2009) and arachidonic acid metabolism coupled to $cPLA_2$ (cytosolic phospholipase A_2; van Rossum et al., 2001; Cho et al., 2011). Indeed, we found that diphenyleneiodonium (DPI; NADPH oxidase inhibitor), AACOCF3 ($cPLA_2$ inhibitor) and methyl arachidonyl fluorophosphonate (MAFP; $cPLA_2$ inhibitor), and nordihydroguaiaretic acid (NDGA; lipoxygenase inhibitor) each attenuated mitotic entry in HeLa cells (Fig. 3, A–D). NADPH oxidase 4 and $cPLA_2$ are localized to the membranes of ER, which accumulates around the centrosome before nuclear breakdown (Whitaker, 2006; Lassègue et al., 2012). It is therefore possible that sources of H_2O_2 are arranged specifically to channel H_2O_2 to the centrosome in mitotic cells.

Mitotic exit phosphatase Cdc14B, but not entry phosphatases Cdc25B and Cdc25C, is sensitive to oxidative inactivation by H_2O_2

The role of H_2O_2 as a signaling molecule that regulates various biological processes has been well established. The best

Downloaded from http://rupress.org/jcb/article-pdf/210/1/23/1590177/jcb_201412068.pdf by guest on 08 February 2026

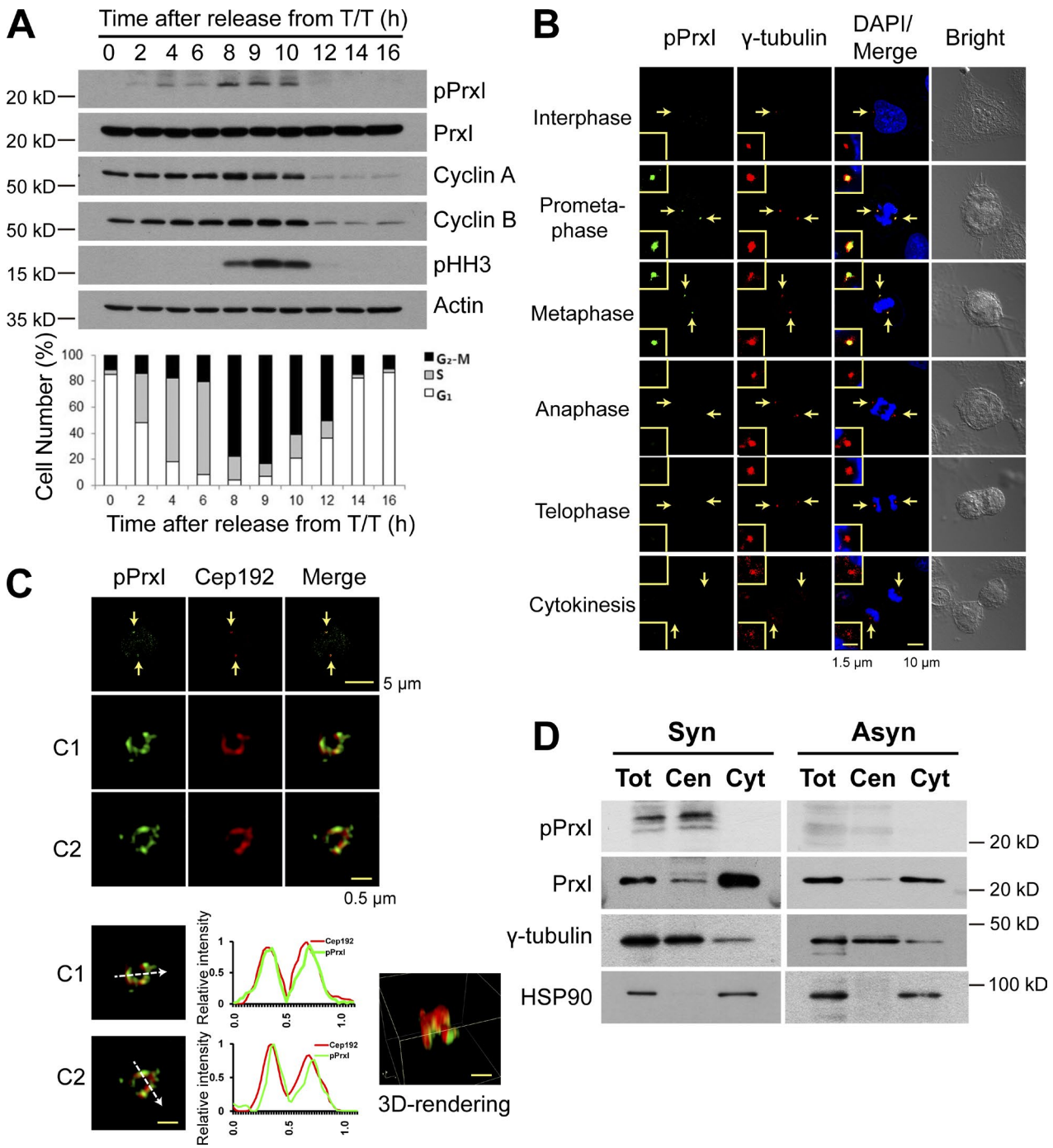

Figure 1. **Phosphorylation of PrxI at Thr^{90} occurs at the centrosome of HeLa cells during early mitosis.** (A, top) HeLa cells that had been arrested at the G_1–S border with a double thymidine block (T/T) were released in fresh medium (at 0 h) and collected at the indicated times for immunoblot analysis with antibodies to the indicated proteins. (bottom) The percentage of cells in the various phases of the cell cycle was estimated by flow cytometric analysis. Data are representative of three experiments with similar results. (B) Confocal microscopy of asynchronously growing HeLa cells stained with antibodies to pPrxI (green) and to γ-tubulin (red). Cell cycle stage was monitored by staining of DNA with DAPI (blue) and bright-field imaging. The areas indicated by the arrows are shown at higher magnification in the insets. (C) 3D-SIM images of pPrxI (green) on two pericentrosomes (C1 and C2) of mitotic HeLa cells. Fluorescent line intensity histograms show the colocalization of pPrxI (green) with pericentrosomal protein Cep192 (red) in two centrosomes. 3D-rendering image is shown in one centrosome. The data shown are from a single representative experiment out of three repeats. Arrows indicate pericentrosomes. (D) HeLa cells synchronized at prometaphase by treatment with thymidine and nocodazole (synchronous [Syn]) or those growing asynchronously (Asyn) were subjected to subcellular fractionation. Total cell lysates without nuclei (Tot) as well as cytosolic (Cyt) and centrosome (Cen) fractions were subjected to immunoblot analysis with antibodies to the indicated proteins.

characterized H_2O_2 effectors are members of the PTP family such as PTP1B and PTEN (phosphatase and tensin homolog), which are reversibly inactivated by H_2O_2 produced in various cells stimulated with growth factors (Kwon et al., 2004; Tonks, 2005; Rhee, 2006). The redox sensitivity of these enzymes is attributable to a low-pK_a cysteine residue located within the PTP

Downloaded from http://rupress.org/jcb/article-pdf/210/1/23/1590177/jcb_201412068.pdf by guest on 08 February 2026

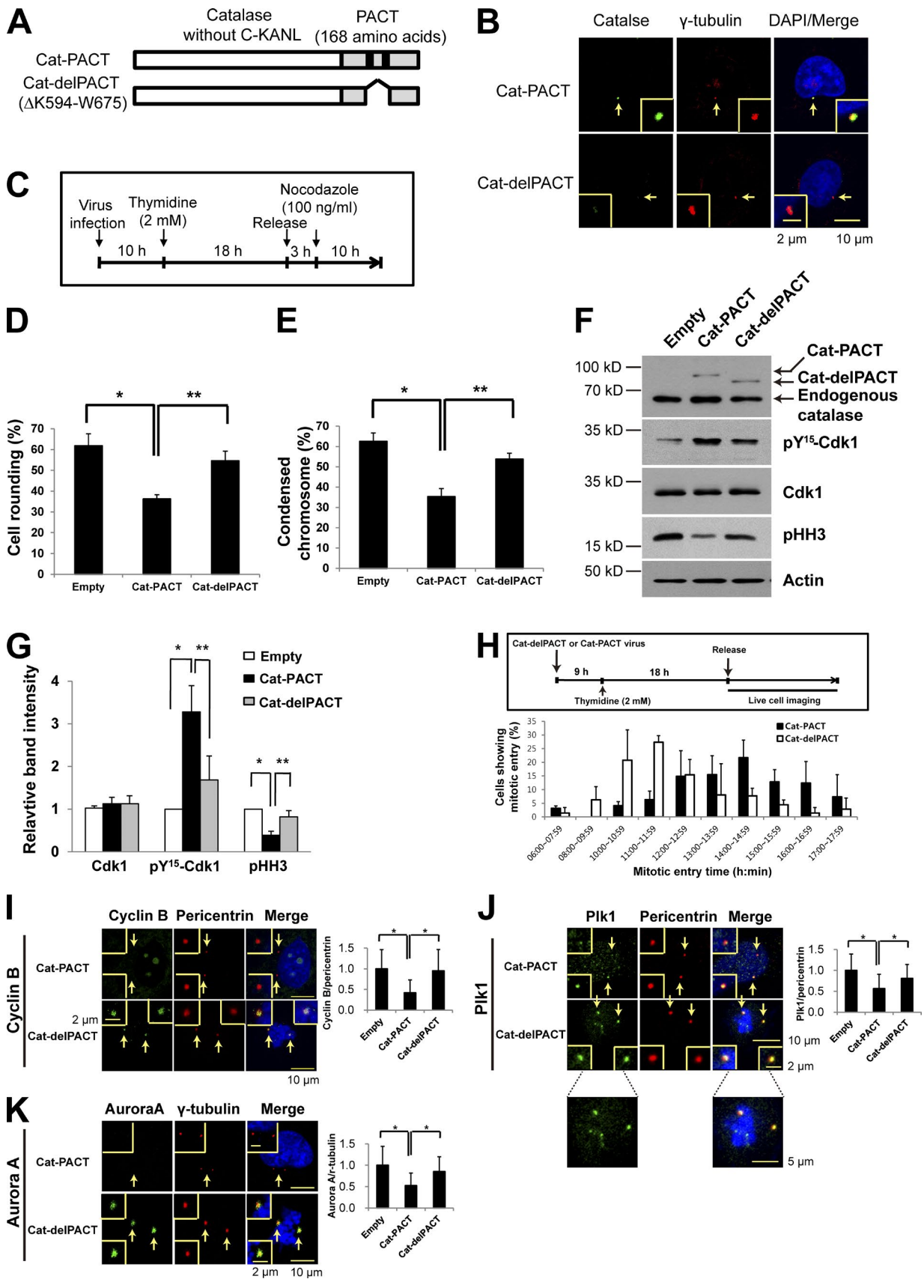

Figure 2. **Effects of centrosome-targeted catalase on mitotic entry and on the abundance of centrosome-associated mitotic regulatory proteins.** (A) Schematic representation of Cat-PACT (in which the centrosome-targeting PACT sequence replaces the C-terminal peroxisome-targeting sequence KANL of catalase) and Cat-delPACT (in which the sequence K594 to W675 of Cat-PACT containing two domains [black boxes] essential for centrosome targeting

Downloaded from http://rupress.org/jcb/article-pdf/210/1/23/1590177/jcb_201412068.pdf by guest on 08 February 2026

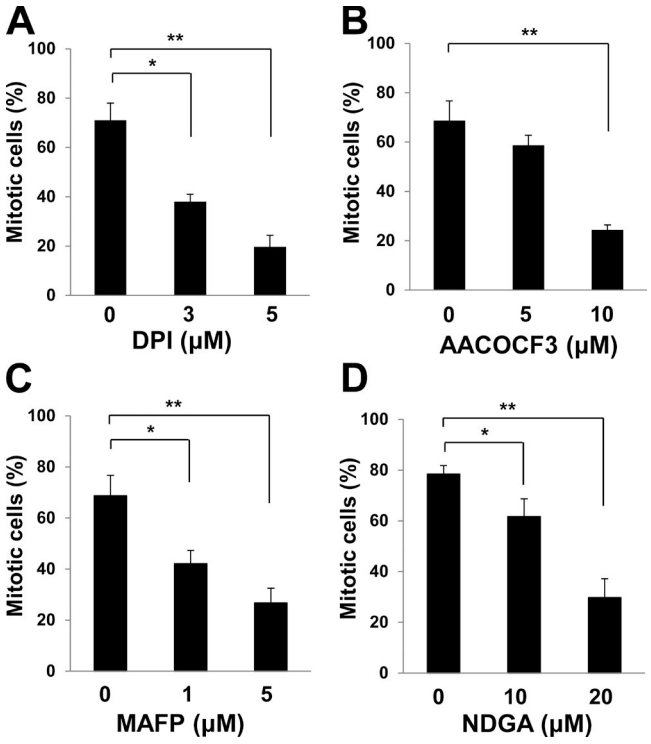

Figure 3. **Sources of H_2O_2 produced during mitotic entry.** (A–D) HeLa cells stably expressing histone H2B–GFP were synchronized at G_1–S by thymidine treatment for 18 h, released into S phase in thymidine-free medium for 3 h, and then incubated in medium containing nocodazole and various concentrations of DPI (A), AACOCF3 (B), MAFP (C), or NDGA (D) for 10 h. The percentage of mitotic cells was then estimated on the basis of chromosome condensation and cell rounding. Data are means ± SD from three independent experiments. *, P < 0.05; **, P < 0.005 (Student's *t* test).

signature motif (HCX_5R). Although PTP1B, PTEN, and Cdc14 act on distinct substrates, they are structurally closely related, whereas Cdc25 phosphatases have a different structure, which is similar to that of rhodanese (Mustelin, 2007).

Oxidation of PTEN renders its structure more compact as a result of the formation of an intramolecular disulfide bond, with the oxidized protein migrating faster than the reduced form during nonreducing SDS-PAGE (Kwon et al., 2004). Like PTEN, Myc-tagged Cdc14B showed a reversible H_2O_2-induced increase in electrophoretic mobility under nonreducing conditions when tested using HeLa cells expressing Myc-tagged Cdc14B (Fig. S2, A and B), whereas no such mobility shift was observed with Myc-tagged forms of Cdc25B or Cdc25C (Fig. S2 B). Cdc14B appeared to be more sensitive to H_2O_2 than was PTEN (Fig. S2 B). Human Cdc14B contains nine Cys residues in addition to the catalytic Cys^{314}. Analysis of various Cys mutants of Cdc14B showed that only Cys^{228} and Cys^{314} among the 10 Cys residues are required for the H_2O_2-dependent mobility shift (Fig. S2 C), suggesting that oxidized Cys^{314} forms a disulfide bond with Cys^{228}.

Although oxidation of Cys residues does not necessarily result in a gel mobility shift, oxidized Cys can be reliably detected by alkylation of reduced Cys residues followed by reduction of the oxidized cysteines and subsequent biotinylation of the newly formed thiols. We applied the biotinylation method to the cells that had been exposed to exogenous H_2O_2 maintained at low micromolar levels by incubation of cells with glucose and glucose oxidase. Such analysis also revealed that Cdc14B and PTEN, but not Cdc25B and Cdc25C, are sensitive to oxidation by H_2O_2 (Fig. S2 D). Collectively, these results suggested that centrosomal Cdc14B might be oxidatively inactivated during early mitosis. Direct evaluation of the oxidation status of centrosomal Cdc14B at different stages of the cell cycle was not possible because biochemical isolation of the centrosome requires treatment with 2-mercaptoethanol (Wu et al., 2008), which would reduce the disulfide bond of oxidized Cdc14B. The redox sensitivity of PP1 and PP2, which contain a redox-sensitive bimetallic center, has also long been described (Rusnak and Reiter, 2000; Pieri et al., 2003; Wright et al., 2009). Nevertheless, their redox regulation in cells has yet to be demonstrated.

Effect of pericentrosomal H_2O_2 on the extent of Cdh1 phosphorylation

The activation of APC/C–Cdh1 has been proposed to occur initially at the centrosome (Raff et al., 2002). Our results suggested that PrxI phosphorylation at the onset of mitosis might give rise to a series of events including an increase in the pericentrosomal concentration of H_2O_2, inactivation of Cdk1-opposing phosphatases and accumulation of phosphorylated Cdh1. To test this hypothesis, we produced rabbit antibodies to the Ser^{40}-phosphorylated form of human Cdh1 (pCdh1). Phosphorylation of Cdh1 is known to occur at as many as 8–11 sites in yeast, *Xenopus laevis*, and mammalian cells (Jaspersen et al., 1999; Kramer et al., 2000). All of these potential Cdk phosphorylation sites were identified indirectly with the use of site-directed mutants. Among them, the amino acid sequence surrounding Ser^{40} in human Cdh1 is best conserved (Fig. S3 A). The specificity of the antibodies was demonstrated using Cdh1 phosphorylated

is deleted). (B) HeLa cells infected with a retroviral vector (pMIN) encoding Cat-PACT or Cat-delPACT were subjected to confocal immunofluorescence microscopy with antibodies to catalase (green) and to γ-tubulin (red). DNA was also stained with DAPI (blue). The area indicated by the arrows (centrosome) is shown at higher magnification in each inset. (C–G) HeLa cells stably expressing GFP-tagged histone H2B were infected with empty, Cat-PACT, or Cat-delPACT retroviral vectors for 10 h in the presence of 6 μg/ml polybrene, treated with (2 mM thymidine) for 18 h, released in fresh medium for 3 h, and then treated with 100 ng/ml nocodazole for 10 h (C). The percentage of mitotic cells was then evaluated on the basis of cell rounding (D) or chromosome condensation (E). Data are means ± SD from three independent experiments (*n* = 50 cells examined for each experiment). *, P < 0.02; **, P < 0.01 (Student's *t* test). The cells were also subjected to immunoblot analysis with antibodies to the indicated proteins (F). The relative immunoblot intensities of Cdk1, pY^{15}-Cdk1, and pHH3 normalized by those of actin were also determined as means ± SD from three independent experiments (G). *, P < 0.05; **, P < 0.005 (Student's *t* test). (H) HeLa cells expressing histone H2B-GFP were infected with Cat-PACT or Cat-delPACT retroviral vectors, synchronized at G_1–S, and released in fresh medium for live-cell imaging. The proportion of cells exhibiting mitotic entry was estimated from Videos 1 and 2 that were acquired over 20 h at 30-min intervals. Data are means ± SD from three independent experiments (*n* = 90 or 70 cells examined in each experiment for Cat-PACT or Cat-delPACT, respectively). (I–K) HeLa cells infected with empty, Cat-PACT, or Cat-delPACT retroviral vectors were treated as in C and then subjected to confocal microscopy with antibodies to cyclin B1 (green) and to pericentrin (red; I), to Plk1 (green) and to pericentrin (red; J), or to Aurora A (green) and to γ-tubulin (red; K). The relative fluorescence intensity ratios of cyclin B1 to pericentrin (I), of Plk1 to pericentrin (J), and of Aurora A to γ-tubulin (K) were also evaluated at the centrosome. The areas indicated by the arrows are shown at higher magnification in the insets. Data are means ± SD from three independent experiments (*n* = 50 cells examined for each experiment). *, P < 0.02 (Student's *t* test).

Downloaded from http://rupress.org/jcb/article-pdf/210/1/23/1590177/jcb_201412068.pdf by guest on 08 February 2026

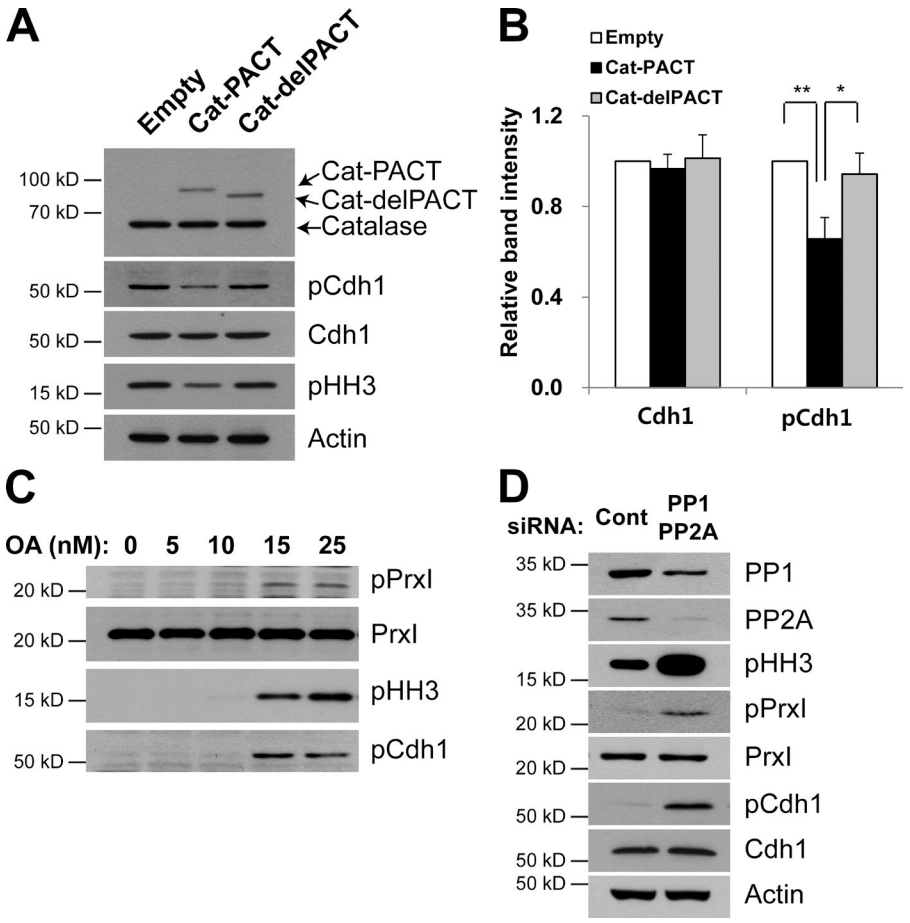

Figure 4. **Effects of centrosome-targeted catalase and OA on Cdh1 phosphorylation and mitotic entry.** (A and B) HeLa cells were infected with empty, Cat-PACT, or Cat-delPACT retroviral vectors and synchronized at prometaphase. Cell lysates were then subjected to immunoblot analysis with antibodies to the indicated proteins (A). The relative immunoblot intensities of Cdh1 and pCdh1 normalized by those of actin were determined as means ± SD from three independent experiments (B). *, $P < 0.05$; **, $P < 0.005$ (Student's *t* test). (C and D) HeLa cells were cultured in the presence of the indicated concentrations of okadaic acid (OA) for 24 h (C) or transiently transfected for 48 h with control siRNA or with a mixtures of siRNAs for PP1, PP2Aα, and PP2Aβ (D), after which cell lysates were subjected to immunoblot analysis with antibodies to the indicated proteins. Data are representative of three experiments with similar results. Cont, control.

by recombinant Cdk1–cyclin B (Fig. S3 B) and Cdh1-depleted HeLa cells (Fig. S3 C). We next examined whether Ser^{40} phosphorylation is important for the binding of Cdh1 to APC/C. HA-tagged forms of wild-type Cdh1 or mutants thereof in which Ser^{40} is replaced with alanine or aspartic acid (S40A or S40D, respectively) were expressed in HeLa cells, and the amount of HA-Cdh1 that coimmunoprecipitated with the APC/C complex was estimated in nocodazole-arrested cells. The amount of coprecipitated S40D (phosphomimetic mutant) was only ∼30% and ∼20% of that of the wild-type or S40A (nonphosphorylatable mutant) proteins, respectively (Fig. S3, D and E), suggesting that Ser^{40} phosphorylation inhibits Cdh1 binding to APC/C.

Using the antibodies to pCdh1, we investigated the effect of Cat-PACT expression on Ser^{40} phosphorylation in nocodazole-arrested cells. The amount of pCdh1 in HeLa cells expressing Cat-PACT was reduced by ∼30% compared with that in cells infected with the empty vector or expressing Cat-delPACT (Fig. 4, A and B), consistent with the notion that Cdh1 phosphorylation is highly influenced by pericentrosomal H_2O_2 level and that pCdh1 undergoes turnover at the centrosome (Raff et al., 2002).

The role of PP1 and PP2A in determining the phosphorylation state of PrxI and Cdh1 was tested in HeLa cells treated with okadaic acid (OA), a potent inhibitor of these phosphatases or silenced for both PP1 and PP2A. The abundance of both pPrxI and pCdh1 was increased by OA treatment (Fig. 4 C) or by silencing PP1 and PP2A (Fig. 4 D), indicating that phosphorylation of PrxI and Cdh1 by Cdk1 is reversed by PP1 and PP2A. Given that Cdc14B is highly concentrated at the centrosome, it is also possible that the OA effect on Cdh1 phosphorylation was mediated indirectly through the inactivation of Cdc14B by H_2O_2 that accumulates around the centrosome as a result of PrxI phosphorylation. As observed before (Picard et al., 1989), OA also promoted mitotic entry as indicated by an increase in the abundance of pHH3 (Fig. 4 C).

A series of events that are proposed to occur at the centrosome in connection to H_2O_2 is shown schematically in Fig. 5, beginning with PrxI phosphorylation. Whereas the intracellular concentration of H_2O_2 increases as the cell cycle progresses to G_2 phase, the centrosome is shielded from the high tide of H_2O_2 by the peroxidase activity of PrxI associated with the organelle. At the onset of mitosis, Cdk1–cyclin B phosphorylates PrxI, which results in exposure of the centrosome to H_2O_2 and consequent inactivation of Cdk1-opposing phosphatases represented by Cdc14B. Among the many Cdk1-phosphorylated proteins in mammalian cells, at least pCdh1 appears to be a substrate of Cdc14B in vitro and in vivo (Bassermann et al., 2008; Schindler and Schultz, 2009; Mocciaro and Schiebel, 2010). In late mitosis, PrxI is dephosphorylated, and the centrosome is consequently again shielded from H_2O_2, allowing sequential reactivation of phosphatases, dephosphorylation of Cdh1, and activation of APC/C-Cdh1. This newly discovered circuit provides a means to integrate input from diverse H_2O_2-generating cellular processes. The presence of PrxI at the centrosome might also serve as a safeguard to prevent unscheduled mitotic entry as a result of an accidental increase in H_2O_2 abundance.

Downloaded from http://rupress.org/jcb/article-pdf/210/1/23/1590177/jcb_201412068.pdf by guest on 08 February 2026

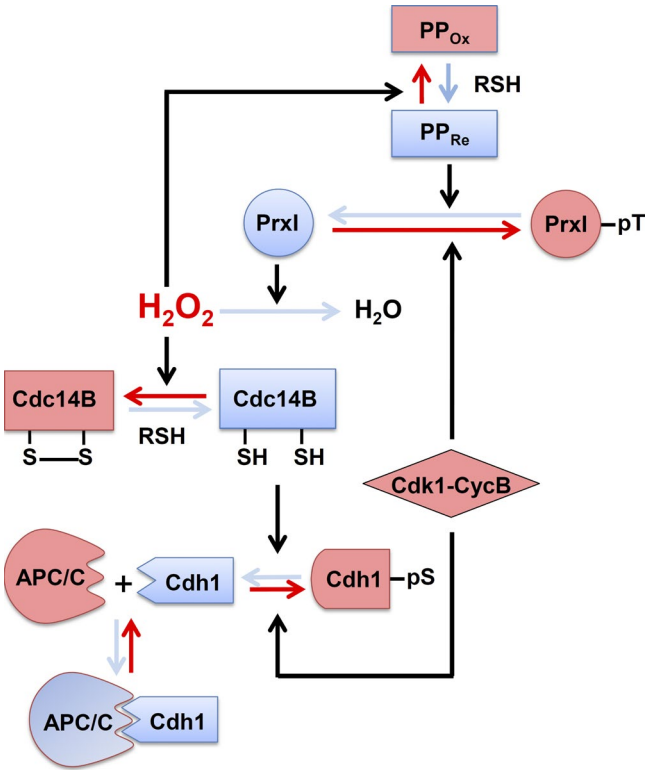

Figure 5. **Proposed scheme for a series of events that result from the phosphorylation or dephosphorylation of PrxI at the centrosome.** Red solid arrows indicate the direction of the reactions resulting from PrxI phosphorylation, whereas the blue arrows indicate the direction of those resulting from PrxI dephosphorylation. Black arrows indicate the reactions catalyzed by the designated enzymes or induced by H_2O_2. PP$_{Ox}$ denotes the oxidized forms of PP1 and PP2A, and PP$_{Re}$ denotes their reduced forms. RSH, thiol-containing reductant such as glutathione or thioredoxin; CycB, cyclin B. See Discussion for details.

Materials and methods

Materials

Nocodazole, *N*-ethylmaleimide (NEM), and TCA were obtained from Sigma-Aldrich; DPI and OA were purchased from EMD Millipore; AACOCF3 was obtained from Santa Cruz Biotechnology, Inc.; and MAFP and NDGA were obtained from Cayman Chemical. Rabbit polyclonal antibodies specific for human PrxI, PrxII, PrxV, or PrxVI were described previously (Kang et al., 1998a,b; Seo et al., 2000), as were those specific for PrxI phosphorylated on Thr^{90} (rabbit IgG; epitope, phosphopeptide CHLAWVNpTPKKQG, which corresponds to residues 83–95 of human Prx I; Chang et al., 2002). Rabbit polyclonal antibodies to Cdc14B, mouse monoclonal antibodies to Plk1, and rabbit antibodies to GFP were obtained from Invitrogen. Antibodies to cyclin A (rabbit IgG; H-432), to cyclin B1 (rabbit IgG; H-20), to Plk1 (mouse IgG; F-8, for immunofluorescence analysis), to HA (mouse IgG; F-7), to Cdk1 (mouse IgG; sc-54), to PP1 (mouse IgG; E-9), and to c-Myc (mouse IgG; 9E10) were obtained from Santa Cruz Biotechnology, Inc. Rabbit monoclonal antibodies to Cdc25C (5H9) and to Aurora A (1G4), rabbit polyclonal antibodies to Tyr^{15}-phosphorylated Cdk1, rabbit monoclonal antibodies to PP2A C subunit (52F8), and mouse antibodies to cyclin B1 (for immunofluorescence analysis) were purchased from Cell Signaling Technology. Antibodies to β-actin (mouse IgG; AC-74) and to γ-tubulin (mouse IgG; GTU-88) were obtained from Sigma-Aldrich, mouse monoclonal antibodies to Cdh1 (Ab-2) were obtained from EMD Millipore, rabbit polyclonal antibodies to Ser^{10}-pHH3 were obtained from EMD Millipore, rabbit monoclonal antibodies to PTEN (C-terminal) were from Epitomics, rabbit antibodies to catalase were from Young In Frontier, rabbit antibodies to pericentrin were obtained from Abcam, and mouse antibodies to HSP90 were obtained from BD. HeLa cells stably expressing histone H2B–GFP (a human histone H2B gene subcloned into pEGFPN1 vector; the expression was driven by the EF-1α promotor, and the vector contained the blasticidin-resistant gene) were provided by J.H. Lee (Ajou University, Suwon, South Korea). The pMIN retrovirus plasmid (a derivative of MPIN plasmid, the entire residual *pol* coding sequence was deleted; Yu et al., 2000) was obtained from Viromed, the pHyPer-Cyto plasmid (catalog no. FP941, cytomegalovirus promoter) was from Evrogen, and pHyPer-C199S (H_2O_2-sentive Cys^{199} was replaced with serine) was described previously (Poburko et al., 2011). MEFs derived from PrxI knockout or catalase knockout mice were prepared at embryonic day 13.5 from embryos obtained by mating PrxI$^{+/-}$ mice (the sequence from exon 1 to exon 6 of a Prx I gene was replaced with the neomycin gene; provided by D.Y. Yu, Korea Research Institute of Biology and Biotechnology, Daejon, South Korea; Han et al., 2012) or Cat$^{+/-}$ mice (the BamHI genomic DNA fragment of the mouse catalase gene, containing parts of intron 4 and exon 5, was replaced by a neomycin resistance cassette in the gene targeting vector; provided by Y.S. Ho, Wayne State University, Detroit, MI; Ho et al., 2004).

Cell culture, transfection, synchronization, and release from the synchronized state

HeLa, U2OS, A431, and MCF7 cells as well as MEFs were cultured in DMEM supplemented with 10% FBS (Gibco) and penicillin-streptomycin (Hyclone). Cell lines were subjected to transient transfection with expression plasmids with the use of the Effectene (QIAGEN) or FuGENE 6 (Roche) reagents, and synthetic siRNAs were introduced into cells with the use of the Oligofectamine reagent (Invitrogen). MEFs were transfected by the Neon transfection method (Invitrogen). Synchronized cells were prepared and released as described previously (Fang et al., 1998; Whitfield et al., 2002), with minor modifications. In brief, for synchronization at the G_1–S border, HeLa cells were grown for 18 h in complete medium containing 2 mM thymidine (Sigma-Aldrich), washed with PBS, incubated for 8 h in fresh medium without thymidine, and cultured again for 18 h in medium containing 2 mM thymidine. The cells were then transferred to fresh medium, and samples were harvested every 1–3 h. For arrest in prometaphase, HeLa cells were treated with 2 mM thymidine for 18 h, released into fresh medium for 3 h, and treated with 100 ng/ml nocodazole (Sigma-Aldrich) for 10 h. The cells were then collected every 0.5–2 h after their transfer to fresh medium. MEFs were synchronized as described previously (García-Higuera et al., 2008), with some modifications. In brief, cells were arrested in G_0 by serum deprivation (0.5% FBS) for 72 h, released in medium containing 10% serum, and in the presence of 0.2 µg/ml aphidicolin (Sigma-Aldrich) for 24 h for G_1–S synchronization, and then treated with 500 ng/ml nocodazole and 5 µM paclitaxel (Sigma-Aldrich) for 12 h for mitotic synchronization.

Plasmids and siRNAs

A full-length Cdc14B cDNA was amplified by PCR from a human testis cDNA library (Takara Bio Inc.). The sequences of PCR primers for the first and second reactions were 5′-CCCCCTGACGGGCCGC-3′ (first, forward), 5′-TTCCTTCAGCTCTGGTCACA-3′ (first, reverse), 5′-AATTGGCCGGCCCATGAAGCGGAAAAGCGAGC-3′ (second, forward), and 5′-ATATGGCGCGCCTTAACGCAAGACTCTTTTAGTC-3′ (second, reverse). The amplified coding region was then cloned into the Fse1 and Asc1 sites of the pCS2-Myc vector (cytomegalovirus pro-

Downloaded from http://rupress.org/jcb/article-pdf/210/1/23/1590177/jcb_201412068.pdf by guest on 08 February 2026

moter, 6 Myc epitope; provided by D. Turner, University of Michigan, Ann Arbor, MI) for expression of a Myc epitope–tagged protein. Point mutations of Cdc14B were generated with the use of a QuikChange Site-Directed Mutagenesis kit (Agilent Technologies) with pCS2-Myc-Cdc14B as the template. The plasmids pCS2-HA-Cdh1(S40A) and pCS2-HA-Cdh1(S40D) were constructed with the same kit and with pCS2-HA-Cdh1 as the template. Mutations were verified by DNA sequencing. Double-stranded siRNA oligonucleotides for PrxI and Cdh1 were synthesized by GE Healthcare and were previously validated (Lee et al., 2011; Song et al., 2011); the target sequences are 5′-AA ACTCAACTGCCAAGTGATT-3′ and 5′-CGCTTGTCTGAGGATT ACG-3′ for PrxI and 5′-GGAACACGCTGACAGGACA-3′ (siCdh1-1) and 5′-GAAGAAGGGTCTGTTCACG-3′ (siCdh1-2) for Cdh1. A control siRNA for GFP (5′-GTTCAGCGTGTCCGGCGAGTT-3′) was obtained from Samchully Pharma. Pan-PP1 siRNA (for the α, β, and γ isoforms; sc-43545) were obtained from Santa Cruz Biotechnology, Inc. Double-stranded siRNA oligonucleotides for PP2A-Cα and PP2A-Cβ were synthesized from GE Healthcare. SMARTpool siRNA target sequences consist of four siRNA targeting multiple sites on PP2A-Cα and PP2A-Cβ. The siRNA sequences for PP2A-Cα are 5′-C CGGAAUGUAGUAACGAUU-3′, 5′-ACAUUAACACCUCGUGAA U-3′, 5′-UCAUGGAACUUGACGAUAC-3′, and 5′-CAGGUAGAG-CUUAAACUAA-3′. The siRNA sequences for PP2A-Cβ are 5′-CA CGAAAGCCGACAAAUUA-3′, 5′-UUUAGUAGAUGGACAGAUA -3′, 5′-CCAGAACGCAUUACAAUAU-3′, and 5′-GAACCAGGCU GCUAUCAUG-3′. Human Cdc25B cDNA (GenBank accession no. BC051711) was obtained from GE Healthcare and cloned into pCS2-Myc, and human His_6-Cdc25C cDNA (plasmid 10964) was obtained from T. Finkel (National Heart, Lung, and Blood Institute, National Institutes of Health, Bethesda, MD) through the Addgene repository.

3D-SIM

Asynchronously growing HeLa cells were fixed with methanol and immunostained with antibodies to pPrxI or with antibodies to Alexa Fluor 647–conjugated Cep 192 C (Kim et al., 2013). SIM image was obtained using a microscope (ELYRA PS.1; Carl Zeiss) with a 63×/1.4 NA objective and an electron-multiplying charge-coupled device (1,024 × 1,024 pixels, 8 × 8–µm pixel size, 65% quantum efficiency; iXon 885; Andor Technology), for a maximum field of view of 80 × 80 µm of the sample. To get line intensity histograms and a 3D-rendering image, acquired images of mitotic HeLa cells were analyzed with Zen software (Carl Zeiss) and NIS elements AR 3.0 software (Nikon).

Expression of Cat-PACT and Cat-delPACT

For generation of the pCat-PACT plasmid, the PACT cDNA was amplified from dsRed-PACT (provided by D.S. Hwang, Seoul National University, Seoul, South Korea) and inserted into a plasmid for human catalase (provided by S.W. Kang, Ewha Woman's University, Seoul, South Korea) from which the DNA sequence encoding the C-terminal KANL residues had been removed. For generation of pCat-delPACT, a region of the PACT sequence (K594–W675) containing two motifs essential for centrosome targeting was removed from pCat-PACT.

Generation of antibodies to Ser^{40}-phosphorylated Cdh1

Rabbits were injected with a keyhole limpet hemocyanin–conjugated phosphopeptide (SPVSpSPSKHG) corresponding to amino acid residues 36–45 of human Cdh1. Antibodies that recognize the nonphosphorylated peptide were removed from serum with the use of an affinity resin conjugated with the nonphosphorylated peptide. Specific antibodies were then further purified with the use of a resin conjugated with the phosphopeptide.

Identification of reduced and oxidized forms of Cdc14B

Reduced and oxidized forms of Cdc14B were identified on the basis of a mobility shift on nonreducing SDS-PAGE as described previously (Kwon et al., 2004), with minor modifications. After treatment with H_2O_2, HeLa cells (10^6 cells) were scraped into 1 ml PBS and mixed with 0.2 ml of ice-cold 50% TCA. The mixture was centrifuged at 2,000 *g* for 5 min at 4°C, and the resulting pellet was washed with ice-cold acetone and then solubilized in 0.2 ml of 100 mM Tris-HCl, pH 6.8, containing 2% SDS and 40 mM NEM. Solubilized proteins (20 µg) were subjected to SDS-PAGE under nonreducing conditions and then transferred to a nitrocellulose membrane for immunoblot analysis with antibodies to Cdc14B or to the Myc epitope tag.

2D-PAGE analysis of PrxI phosphorylated on Thr^{90}

Recombinant human PrxI was expressed in and purified from bacteria as previously described (Seo et al., 2000). Complementary DNA corresponding to PrxI protein was expressed in *Escherichia coli* and PrxI was purified by ammonium sulfate fractionation (40–60% saturation) and sequential chromatography on DEAE-Sephacel ion exchange and HPLC TSK heparin-5PW columns. The protein (10 µg) was phosphorylated by incubation for 1 h at 37°C with 8 µg Cdk1–cyclin B (New England Biolabs, Inc.) in a final volume of 50 µl of a solution containing 50 mM Tris-HCl, pH 7.5, 10 mM $MgCl_2$, 1 mM EGTA, 1 mM DTT, and 200 µM ATP. One-half of the product was used to estimate the proportion of Thr^{90}-phosphorylated PrxI by 2D-PAGE analysis, and the other half was used as a standard for the quantification of pPrxI in lysates of mitotic HeLa cells.

Detection of oxidized Cdc14B and PTEN with a biotinylation assay

For detection of Cdc14B oxidation in Fig. 5 D, an enhanced method based on Cys biotinylation was performed as previously described (Kwon et al., 2004), with some modifications. In brief, cells (10^6 per 100-mm dish) exposed to glucose oxidase in high-glucose medium were washed with ice-cold PBS, scraped into 1 ml of the same solution, transferred to a microfuge tube, isolated by centrifugation at 8,000 *g* for 1 min at 4°C, and rapidly frozen in liquid nitrogen. The frozen cells were incubated for 1 h at room temperature with 1 ml of oxygen-free extraction buffer (50 mM sodium phosphate, pH 7.0, 1 mM EDTA, 10 mM NEM, 10 mM iodoacetic acid, 1% Triton X-100, 5 mM NaF, 50 µg/ml leupeptin, 50 µg/ml aprotinin, and 1 mM 4-(2-aminoethyl) benzene-sulfonyl fluoride) in an anaerobic chamber. The samples were then centrifuged, SDS was added to the harvested supernatants to a final concentration of 1%, and the mixtures were incubated for 2 h at room temperature in the dark. 500-µg portions of the denatured proteins were precipitated by the addition of TCA to a final concentration of 10% and incubation for 1 h at room temperature. The precipitates were washed twice with acetone that had been cooled on dry ice and were then reduced by incubation for 30 min at 50°C in 0.1 ml of oxygen-free reducing buffer (50 mM Hepes-NaOH, pH 7.7, 1 mM EDTA, 2% SDS, and 4 mM DTT) in an anaerobic chamber. The reduced proteins containing free sulfhydryl groups were biotinylated by incubation for 30 min at 50°C with 0.9 ml of a solution containing 50 mM sodium phosphate, pH 7.0, 1 mM EDTA, and 1 mM biotin that had been conjugated to polyethylene oxide–maleimide (Thermo Fisher Scientific). The reaction was stopped by the addition of DTT to a final concentration of 1 mM, and proteins were precipitated by incubation with TCA at a final concentration of 10% for 1 h. The precipitates were washed with dry ice–chilled acetone and then solubilized in 0.2 ml of a solution containing 50 mM Hepes-NaOH, pH 7.7, 1 mM EDTA, and 2% SDS, with ultrasonic treatment for 15 s. The samples were diluted with 0.2 ml of the same solution without SDS, and 40-µl portions of the resulting mixtures were saved for immunoblot analysis. The remaining

Downloaded from http://rupress.org/jcb/article-pdf/210/1/23/1590177/jcb_201412068.pdf by guest on 08 February 2026

360-µl portion of each mixture was diluted further with the same solution without SDS until the final concentration of SDS was 0.5%. Biotinylated proteins were then precipitated by incubation for 1 h at room temperature with 3 µl of packed UltraLink Immobilized NeutrAvidin (Thermo Fisher Scientific). The beads were washed five times with a solution containing 20 mM Hepes-NaOH, pH 7.7, 200 mM NaCl, 1 mM EDTA, and 0.5% SDS, and the biotinylated proteins were released from the beads by boiling in SDS-PAGE sample buffer and then subjected to immunoblot analysis with antibodies to Cdc14B. Biotinylated PTEN was detected on the stripped blots with antibodies to PTEN.

Preparation of total cell lysates without nuclei as well as cytosolic and centrosome fractions

Subcellular fractionation was performed as described previously (Bornens et al., 1987), with minor modifications. Prometaphase-arrested HeLa cells (10^7) obtained by treatment with thymidine and nocodazole were lysed in 5 ml of a hypotonic solution (1 mM Hepes-NaOH, pH 7.2, 0.5% NP-40, 0.5 mM $MgCl_2$, 0.1% 2-mercaptoethanol, proteinase inhibitor cocktail, 50 mM NaF, and 1 mM sodium orthovanadate). The cell lysate was centrifuged at 2,500 *g* for 10 min at 4°C to remove nuclei and debris, and the resulting supernatant was collected and filtered through a 50-µm nylon mesh for analysis as a total cell lysate without nuclei. Hepes and DNase were added to a portion of the latter preparation to final concentrations of 10 mM and 2 U/ml, respectively, and the mixture was incubated for 30 min on ice before layering on top of 0.5 ml of a solution containing 60% (wt/wt) sucrose, 10 mM Pipes-NaOH, pH 7.2, 0.1% Triton X-100, and 0.1% 2-mercaptoethanol in a 5-ml centrifuge tube. The gradient was centrifuged at 10,000 *g* for 30 min at 4°C, after which the bottom portion (1.5 ml) containing centrosomes was purified further by layering on top of a discontinuous sucrose gradient consisting of 0.5 ml of 70%, 0.3 ml of 50%, and 0.3 ml of 40% sucrose in the same solution followed by centrifugation at 120,000 *g* for 1 h at 4°C. 0.2-ml fractions were collected from the bottom of the tube, diluted with 1 ml of 10 mM Pipes-NaOH, pH 7.2, and centrifuged at 15,000 *g* for 10 min at 4°C. The resulting pellets were subjected to immunoblot analysis with antibodies to γ-tubulin and to HSP90. The two fractions containing the largest amounts of γ-tubulin were pooled and used as the centrosomal fraction. The final four fractions containing the largest amounts of HSP90 were pooled and used as the cytosolic fraction.

Flow cytometry

For analysis of cell cycle stage, cells (5×10^5/ml) were washed twice with ice-cold PBS, fixed overnight at 4°C in 70% ethanol, and stained with 1 ml of a solution containing 50 µg/ml RNase and 50 µg/ml propidium iodide before flow cytometry with a FACSCalibur instrument (BD).

Immunofluorescence analysis and live-cell imaging

Cells were cultured in 12-well dishes containing coverslips (diameter, 12 mm) coated with poly-L-lysine for both live-cell imaging and immunofluorescence staining. For the latter, the cells were fixed for 10 min on ice in 100% methanol or 4% formaldehyde in PBS, exposed for 30 min at room temperature to PBS containing 5% horse serum (Gibco-BRL) and 0.1% Triton X-100, and then incubated for 30 min at room temperature with primary antibodies to phosphorylated PrxI, to cyclin B1, to Plk1, or to Aurora A in the same solution. After three 5-min washes with PBS, the cells were incubated for 30 min at room temperature with Alexa Fluor 488–conjugated goat secondary antibodies (Invitrogen) at a 1:1,000 dilution in PBS containing 5% horse serum and 0.1% Triton X-100. For coimmunostaining of a centrosome marker, the cells were again washed three times with PBS, exposed for 30 min to PBS containing 5% horse serum and 0.1% Triton X-100, and incubated for 30 min with primary antibodies to γ-tubulin or to pericentrin in the same solution before detection of immune complexes with Alexa Fluor 546–conjugated goat secondary antibodies (Invitrogen) at a 1:500 dilution. The cells were also stained with 0.2 µg/ml DAPI to detect DNA. Confocal images were acquired using a 60× Plan Apochromat VC objective, NA 1.40, by illuminating with a 488-nm multi-Ar laser (for excitation of Alexa Fluor 488 fluorochrome) or with a 561-nm diode-pumped solid-state laser (for excitation of Alexa Fluor 546 fluorochrome) with a microscope (A1R; Nikon) equipped with galvano detector, and images were processed with NIS elements AR 3.0 software. For live-cell imaging, cells were maintained in an incubation chamber (Chamlide TC; Live Cell Instrument) at 37°C under an atmosphere of 5% CO_2 in air.

Binding of Cdh1 to the APC/C complex in HeLa cells

HeLa cells (3×10^6) transiently expressing HA-tagged wild-type or mutant (S40D or S40A) forms of human Cdh1 were synchronized at prometaphase by treatment with thymidine and nocodazole. The cells were then lysed by ultrasonic treatment in 1 ml of a solution containing 50 mM Tris-HCl, pH 7.7, 150 mM NaCl, 0.5% NP-40, 1 mM DTT, a proteinase inhibitor cocktail, 50 mM NaF, and 0.5 µM OA, the lysates were centrifuged at 15,000 *g* for 30 min at 4°C, and the resulting supernatants (800 µl) were incubated for 4 h at 4°C with 10 µl of protein A–conjugated beads that had been coated with 10 µg of antibodies to Cdc27 (H-300; Santa Cruz Biotechnology, Inc.). The beads were then washed five times with the cell lysis buffer containing 500 mM NaCl and twice with the original lysis buffer, after which bound proteins were eluted with SDS sample buffer and subjected to immunoblot analysis.

Statistical analysis

Quantitative data are presented as means ± SD (unless indicated otherwise) and were analyzed with Student's *t* test. A $P < 0.05$ was considered statistically significant.

Online supplemental material

Fig. S1 demonstrates phosphorylation of PrxI on Thr^{90} at the centrosome of mitotic cells. Fig. S2 shows the sensitivity of PTPs to H_2O_2. Fig. S3 shows identification of a potential Cdk phosphorylation site in Cdh1. Videos 1 and 2 show live-cell imaging of HeLa cells expressing histone H2B-GFP and Cat-delPACT or histone H2B–GFP and Cat-PACT, respectively. Online supplemental material is available at http://www.jcb.org/cgi/content/full/jcb.201412068/DC1. Additional data are available in the JCB DataViewer at http://dx.doi.org/10.1083/jcb.201412068.dv.

Acknowledgments

We thank Jung-Eun Park at the National Cancer Institute (Bethesda, MD) for providing all the technical assistance for SIM imaging.

This study was supported by grants from the Korean Science and Engineering Foundation (National Honor Scientist program grant 2006-05106 and BioR&D program grant M10642040001-07N4204-00110 to S.G. Rhee) and the National Research Foundation of Korea (Basic Science Research program grants 2011-0010514 and 2012R1A1A2002268 to D. Kang).

The authors declare no competing financial interests.

Author contributions: D. Kang and S.G. Rhee conceived the study and supervised experiments. J.M. Lim, H.A. Woo, and D. Kang performed experiments and analyzed data. K.S. Lee provided critical reagents. D. Kang and S.G. Rhee wrote the paper. All authors discussed and commented on the manuscript.

Downloaded from http://rupress.org/jcb/article-pdf/210/1/23/1590177/jcb_201412068.pdf by guest on 08 February 2026

Submitted: 26 December 2014
Accepted: 27 May 2015

References

Bassermann, F., D. Frescas, D. Guardavaccaro, L. Busino, A. Peschiaroli, and M. Pagano. 2008. The Cdc14B-Cdh1-Plk1 axis controls the G2 DNA-damage-response checkpoint. *Cell.* 134:256–267. http://dx.doi.org/10.1016/j.cell.2008.05.043

Bonnet, J., P. Coopman, and M.C. Morris. 2008. Characterization of centrosomal localization and dynamics of Cdc25C phosphatase in mitosis. *Cell Cycle.* 7:1991–1998. http://dx.doi.org/10.4161/cc.7.13.6095

Bornens, M., M. Paintrand, J. Berges, M.C. Marty, and E. Karsenti. 1987. Structural and chemical characterization of isolated centrosomes. *Cell Motil. Cytoskeleton.* 8:238–249. http://dx.doi.org/10.1002/cm.970080305

Chang, T.S., W. Jeong, S.Y. Choi, S. Yu, S.W. Kang, and S.G. Rhee. 2002. Regulation of peroxiredoxin I activity by Cdc2-mediated phosphorylation. *J. Biol. Chem.* 277:25370–25376. http://dx.doi.org/10.1074/jbc.M110432200

Cho, H.P., Y. Liu, M. Gomez, J. Dunlap, M. Tyers, and Y. Wang. 2005. The dual-specificity phosphatase CDC14B bundles and stabilizes microtubules. *Mol. Cell. Biol.* 25:4541–4551. http://dx.doi.org/10.1128/MCB.25.11.4541-4551.2005

Cho, K.J., J.M. Seo, and J.H. Kim. 2011. Bioactive lipoxygenase metabolites stimulation of NADPH oxidases and reactive oxygen species. *Mol. Cells.* 32:1–5. http://dx.doi.org/10.1007/s10059-011-1021-7

Domingo-Sananes, M.R., O. Kapuy, T. Hunt, and B. Novak. 2011. Switches and latches: a biochemical tug-of-war between the kinases and phosphatases that control mitosis. *Philos. Trans. R. Soc. Lond. B Biol. Sci.* 366:3584–3594. http://dx.doi.org/10.1098/rstb.2011.0087

Fang, G., H. Yu, and M.W. Kirschner. 1998. Direct binding of CDC20 protein family members activates the anaphase-promoting complex in mitosis and G1. *Mol. Cell.* 2:163–171. http://dx.doi.org/10.1016/S1097-2765(00)80126-4

García-Higuera, I., E. Manchado, P. Dubus, M. Cañamero, J. Méndez, S. Moreno, and M. Malumbres. 2008. Genomic stability and tumour suppression by the APC/C cofactor Cdh1. *Nat. Cell Biol.* 10:802–811. http://dx.doi.org/10.1038/ncb1742

Gillingham, A.K., and S. Munro. 2000. The PACT domain, a conserved centrosomal targeting motif in the coiled-coil proteins AKAP450 and pericentrin. *EMBO Rep.* 1:524–529. http://dx.doi.org/10.1093/embo-reports/kvd105

Han, Y.H., T. Kwon, S.U. Kim, H.L. Ha, T.H. Lee, J.M. Kim, E.K. Jo, B.Y. Kim, Y. Yoon do, and D.Y. Yu. 2012. Peroxiredoxin I deficiency attenuates phagocytic capacity of macrophage in clearance of the red blood cells damaged by oxidative stress. *BMB Rep.* 45:560–564. http://dx.doi.org/10.5483/BMBRep.2012.45.10.082

Havens, C.G., A. Ho, N. Yoshioka, and S.F. Dowdy. 2006. Regulation of late G1/S phase transition and APC Cdh1 by reactive oxygen species. *Mol. Cell. Biol.* 26:4701–4711. http://dx.doi.org/10.1128/MCB.00303-06

Ho, Y.S., Y. Xiong, W. Ma, A. Spector, and D.S. Ho. 2004. Mice lacking catalase develop normally but show differential sensitivity to oxidant tissue injury. *J. Biol. Chem.* 279:32804–32812. http://dx.doi.org/10.1074/jbc.M404800200

Jackman, M., C. Lindon, E.A. Nigg, and J. Pines. 2003. Active cyclin B1-Cdk1 first appears on centrosomes in prophase. *Nat. Cell Biol.* 5:143–148. http://dx.doi.org/10.1038/ncb918

Jaspersen, S.L., J.F. Charles, and D.O. Morgan. 1999. Inhibitory phosphorylation of the APC regulator Hct1 is controlled by the kinase Cdc28 and the phosphatase Cdc14. *Curr. Biol.* 9:227–236. http://dx.doi.org/10.1016/S0960-9822(99)80111-0

Kang, S.W., I.C. Baines, and S.G. Rhee. 1998a. Characterization of a mammalian peroxiredoxin that contains one conserved cysteine. *J. Biol. Chem.* 273:6303–6311. http://dx.doi.org/10.1074/jbc.273.11.6303

Kang, S.W., H.Z. Chae, M.S. Seo, K. Kim, I.C. Baines, and S.G. Rhee. 1998b. Mammalian peroxiredoxin isoforms can reduce hydrogen peroxide generated in response to growth factors and tumor necrosis factor-α. *J. Biol. Chem.* 273:6297–6302. http://dx.doi.org/10.1074/jbc.273.11.6297

Kim, T.S., J.E. Park, A. Shukla, S. Choi, R.N. Murugan, J.H. Lee, M. Ahn, K. Rhee, J.K. Bang, B.Y. Kim, et al. 2013. Hierarchical recruitment of Plk4 and regulation of centriole biogenesis by two centrosomal scaffolds, Cep192 and Cep152. *Proc. Natl. Acad. Sci. USA.* 110:E4849–E4857. http://dx.doi.org/10.1073/pnas.1319656110

Kramer, E.R., N. Scheuringer, A.V. Podtelejnikov, M. Mann, and J.M. Peters. 2000. Mitotic regulation of the APC activator proteins CDC20 and CDH1. *Mol. Biol. Cell.* 11:1555–1569. http://dx.doi.org/10.1091/mbc.11.5.1555

Kwon, J., S.R. Lee, K.S. Yang, Y. Ahn, Y.J. Kim, E.R. Stadtman, and S.G. Rhee. 2004. Reversible oxidation and inactivation of the tumor suppressor PTEN in cells stimulated with peptide growth factors. *Proc. Natl. Acad. Sci. USA.* 101:16419–16424. http://dx.doi.org/10.1073/pnas.0407396101

Lassègue, B., A. San Martín, and K.K. Griendling. 2012. Biochemistry, physiology, and pathophysiology of NADPH oxidases in the cardiovascular system. *Circ. Res.* 110:1364–1390. http://dx.doi.org/10.1161/CIRCRESAHA.111.243972

Leach, C., S. Shenolikar, and D.L. Brautigan. 2003. Phosphorylation of phosphatase inhibitor-2 at centrosomes during mitosis. *J. Biol. Chem.* 278:26015–26020. http://dx.doi.org/10.1074/jbc.M300782200

Lee, K.W., D.J. Lee, J.Y. Lee, D.H. Kang, J. Kwon, and S.W. Kang. 2011. Peroxiredoxin II restrains DNA damage-induced death in cancer cells by positively regulating JNK-dependent DNA repair. *J. Biol. Chem.* 286:8394–8404. http://dx.doi.org/10.1074/jbc.M110.179416

Lindqvist, A., V. Rodríguez-Bravo, and R.H. Medema. 2009. The decision to enter mitosis: feedback and redundancy in the mitotic entry network. *J. Cell Biol.* 185:193–202. http://dx.doi.org/10.1083/jcb.200812045

Mocciaro, A., and E. Schiebel. 2010. Cdc14: a highly conserved family of phosphatases with non-conserved functions? *J. Cell Sci.* 123:2867–2876. http://dx.doi.org/10.1242/jcs.074815

Mochida, S., S. Ikeo, J. Gannon, and T. Hunt. 2009. Regulated activity of PP2A-B55 delta is crucial for controlling entry into and exit from mitosis in *Xenopus* egg extracts. *EMBO J.* 28:2777–2785. http://dx.doi.org/10.1038/emboj.2009.238

Mustelin, T. 2007. A brief introduction to the protein phosphatase families. *Methods Mol. Biol.* 365:9–22.

Pesin, J.A., and T.L. Orr-Weaver. 2008. Regulation of APC/C activators in mitosis and meiosis. *Annu. Rev. Cell Dev. Biol.* 24:475–499. http://dx.doi.org/10.1146/annurev.cellbio.041408.115949

Peters, J.M. 2006. The anaphase promoting complex/cyclosome: a machine designed to destroy. *Nat. Rev. Mol. Cell Biol.* 7:644–656. http://dx.doi.org/10.1038/nrm1988

Picard, A., J.P. Capony, D.L. Brautigan, and M. Dorée. 1989. Involvement of protein phosphatases 1 and 2A in the control of M phase-promoting factor activity in starfish. *J. Cell Biol.* 109:3347–3354. http://dx.doi.org/10.1083/jcb.109.6.3347

Pieri, L., S. Dominici, B. Del Bello, E. Maellaro, M. Comporti, A. Paolicchi, and A. Pompella. 2003. Redox modulation of protein kinase/phosphatase balance in melanoma cells: the role of endogenous and γ-glutamyltransferase-dependent H2O2 production. *Biochim. Biophys. Acta.* 1621:76–83. http://dx.doi.org/10.1016/S0304-4165(03)00048-5

Poburko, D., J. Santo-Domingo, and N. Demaurex. 2011. Dynamic regulation of the mitochondrial proton gradient during cytosolic calcium elevations. *J. Biol. Chem.* 286:11672–11684. http://dx.doi.org/10.1074/jbc.M110.159962

Raff, J.W., K. Jeffers, and J.Y. Huang. 2002. The roles of Fzy/Cdc20 and Fzr/Cdh1 in regulating the destruction of cyclin B in space and time. *J. Cell Biol.* 157:1139–1149. http://dx.doi.org/10.1083/jcb.200203035

Rhee, S.G. 2006. Cell signaling. H2O2, a necessary evil for cell signaling. *Science.* 312:1882–1883. http://dx.doi.org/10.1126/science.1130481

Rhee, S.G., H.A. Woo, I.S. Kil, and S.H. Bae. 2012. Peroxiredoxin functions as a peroxidase and a regulator and sensor of local peroxides. *J. Biol. Chem.* 287:4403–4410. http://dx.doi.org/10.1074/jbc.R111.283432

Rusnak, F., and T. Reiter. 2000. Sensing electrons: protein phosphatase redox regulation. *Trends Biochem. Sci.* 25:527–529. http://dx.doi.org/10.1016/S0968-0004(00)01659-5

Schindler, K., and R.M. Schultz. 2009. CDC14B acts through FZR1 (CDH1) to prevent meiotic maturation of mouse oocytes. *Biol. Reprod.* 80:795–803. http://dx.doi.org/10.1095/biolreprod.108.074906

Schmitz, M.H., M. Held, V. Janssens, J.R. Hutchins, O. Hudecz, E. Ivanova, J. Goris, L. Trinkle-Mulcahy, A.I. Lamond, I. Poser, et al. 2010. Live-cell imaging RNAi screen identifies PP2A-B55alpha and importin-beta1 as key mitotic exit regulators in human cells. *Nat. Cell Biol.* 12:886–893. http://dx.doi.org/10.1038/ncb2092

Seo, M.S., S.W. Kang, K. Kim, I.C. Baines, T.H. Lee, and S.G. Rhee. 2000. Identification of a new type of mammalian peroxiredoxin that forms an intramolecular disulfide as a reaction intermediate. *J. Biol. Chem.* 275:20346–20354. http://dx.doi.org/10.1074/jbc.M001943200

Song, M.S., A. Carracedo, L. Salmena, S.J. Song, A. Egia, M. Malumbres, and P.P. Pandolfi. 2011. Nuclear PTEN regulates the APC-CDH1 tumor-suppressive complex in a phosphatase-independent manner. *Cell.* 144:187–199. http://dx.doi.org/10.1016/j.cell.2010.12.020

Tonks, N.K. 2005. Redox redux: revisiting PTPs and the control of cell signaling. *Cell.* 121:667–670. http://dx.doi.org/10.1016/j.cell.2005.05.016

Downloaded from http://rupress.org/jcb/article-pdf/210/1/23/1590177/jcb_201412068.pdf by guest on 08 February 2026

van Leuken, R., L. Clijsters, and R. Wolthuis. 2008. To cell cycle, swing the APC/C. *Biochim. Biophys. Acta.* 1786:49–59.

van Rossum, G.S., A.S. Vlug, H. van den Bosch, A.J. Verkleij, and J. Boonstra. 2001. Cytosolic phospholipase A(2) activity during the ongoing cell cycle. *J. Cell. Physiol.* 188:321–328. http://dx.doi.org/10.1002/jcp.1123

Whitaker, M. 2006. Calcium microdomains and cell cycle control. *Cell Calcium.* 40:585–592. http://dx.doi.org/10.1016/j.ceca.2006.08.018

Whitfield, M.L., G. Sherlock, A.J. Saldanha, J.I. Murray, C.A. Ball, K.E. Alexander, J.C. Matese, C.M. Perou, M.M. Hurt, P.O. Brown, and D. Botstein. 2002. Identification of genes periodically expressed in the human cell cycle and their expression in tumors. *Mol. Biol. Cell.* 13:1977–2000. http://dx.doi.org/10.1091/mbc.02-02-0030.

Wright, V.P., P.J. Reiser, and T.L. Clanton. 2009. Redox modulation of global phosphatase activity and protein phosphorylation in intact skeletal muscle. *J. Physiol.* 587:5767–5781. http://dx.doi.org/10.1113/jphysiol.2009.178285

Wu, J., H.P. Cho, D.B. Rhee, D.K. Johnson, J. Dunlap, Y. Liu, and Y. Wang. 2008. Cdc14B depletion leads to centriole amplification, and its overexpression prevents unscheduled centriole duplication. *J. Cell Biol.* 181:475–483. http://dx.doi.org/10.1083/jcb.200710127

Wu, J.Q., J.Y. Guo, W. Tang, C.S. Yang, C.D. Freel, C. Chen, A.C. Nairn, and S. Kornbluth. 2009. PP1-mediated dephosphorylation of phosphoproteins at mitotic exit is controlled by inhibitor-1 and PP1 phosphorylation. *Nat. Cell Biol.* 11:644–651. http://dx.doi.org/10.1038/ncb1871

Wurzenberger, C., and D.W. Gerlich. 2011. Phosphatases: providing safe passage through mitotic exit. *Nat. Rev. Mol. Cell Biol.* 12:469–482. http://dx.doi.org/10.1038/nrm3149

Yamaura, M., J. Mitsushita, S. Furuta, Y. Kiniwa, A. Ashida, Y. Goto, W.H. Shang, M. Kubodera, M. Kato, M. Takata, et al. 2009. NADPH oxidase 4 contributes to transformation phenotype of melanoma cells by regulating G2-M cell cycle progression. *Cancer Res.* 69:2647–2654. http://dx.doi.org/10.1158/0008-5472.CAN-08-3745

Yu, S.S., J.M. Kim, and S. Kim. 2000. High efficiency retroviral vectors that contain no viral coding sequences. *Gene Ther.* 7:797–804. http://dx.doi.org/10.1038/sj.gt.3301164

Downloaded from http://rupress.org/jcb/article-pdf/210/1/23/1590177/jcb_201412068.pdf by guest on 08 February 2026